J|A|C|S
ARTICLES
Published on Web 04/16/2005

Charge Separation and Efficient Light Energy Conversion in Sensitized Mesoscopic Solar Cells Based on Binary Ionic Liquids

Peng Wang,[†,§] Bernard Wenger,[†] Robin Humphry-Baker,[†] Jacques-E. Moser,[†] Joël Teuscher,[†] Willi Kantlehner,[‡] Jochen Mezger,[‡] Edmont V. Stoyanov,[‡] Shaik M. Zakeeruddin,*[,†] and Michael Grätzel*[,†]

Contribution from the Laboratory for Photonics and Interfaces, Swiss Federal Institute of Technology, CH-1015 Lausanne, Switzerland, and FB Chemie/Organische Chemie, FH Aalen, 73430 Aalen, Germany

Received December 24, 2004; E-mail: shaik.zakeer@epfl.ch; michael.graetzel@epfl.ch

Abstract: A 7.4% power conversion efficiency at air mass (AM) 1.5 full sunlight was reached with a mesoscopic solar cell employing a new binary ionic liquid electrolyte composed of 1-propyl-3-methylimidazolium iodide and 1-ethyl-3-methylimidazolium tricyanomethanide in conjunction with the amphiphilic ruthenium complex NaRu(4-carboxylic acid-4′-carboxylate)(4,4′-dinonyl-2,2′-bipyridine)$(NCS)_2$, coded as Z-907Na. Ultramicroelectrode voltammetric, nanosecond laser transient absorbance, and photovoltaic measurements show that a high iodide concentration is required for dye regeneration to compete efficiently with charge recombination. A surprisingly fast reductive quenching process is turned on in pure iodide melts. This channel is unproductive, explaining the lower photocurrents observed under these conditions.

Introduction

The first successful demonstration of a nanocrytalline dye-sensitized solar cell (DSC) in 1991 introduced an innovative approach for low-cost alternatives to traditional inorganic photovoltaic devices.[1] The employed mesoscopic TiO_2 film texture enhances greatly the light-harvesting efficiency of surface-anchored sensitizer molecules. Ultrafast electron injection from the photoexcited dye into the conduction band of TiO_2 is followed by dye regeneration and transportation of the oxidized form of redox mediator (or hole) to the counter electrode.[2,3] A DSC using the well-known N-3 sensitizer[4] now achieves 11% power conversion efficiency[5] following optimization of the electrolyte[6] and of the meososcopic structure of the TiO_2 film.[7] However these systems employ a volatile electrolyte mainly composed of acetonitrile, whose encapsulation at elevated temperature is a major challenge in view of practical industrial applications.

The significance of using the amphiphilic polypyridyl ruthenium sensitizer coded as Z-907 to maintain stability of the DSC under prolonged thermal stress was demonstrated in 2003.[8,9] Another important condition to reach this goal was the use of methoxyproprionitrile (MPN)-based electrolytes that did not contain any lithium ions. Other superior features of Z-907 in comparison to the N-3 sensitizer have been demonstrated, e.g., in devices with some ionic liquid electrolytes,[10] the cobalt-(II/III) redox couples,[11] and solid hole transport materials.[12]

For practical applications and to lower the cost of photovoltaic power production, a substantial improvement in device ef-

[†] Swiss Federal Institute of Technology.
[‡] FH Aalen.
[§] Present address: Cavendish Laboratory, University of Cambridge, Madingley Rd., Cambridge CB3 0HE, U.K.

(1) O'Regan, B.; Grätzel, M. *Nature* **1991**, *353*, 737.
(2) (a) Hagfeldt, A.; Grätzel, M. *Acc. Chem. Res*. **2000**, *33*, 269. (b) Grätzel, M. *Nature* **2001**, *414*, 338.
(3) (a) Dang, X.; Hupp, J. T. *J. Am. Chem. Soc*. **1999**, *121*, 8399. (b) Bach, U.; Tachibana, Y.; Moser, J.-E.; Haque, S. A.; Durrant, J. R.; Grätzel, M.; Klug, D. R. *J. Am. Chem. Soc*. **1999**, *121*, 7445. (c) Sapp, S. A.; Elliott, C. M.; Contado, C.; Caramori, S.; Bignozzi, C. A. *J. Am. Chem. Soc*. **2002**, *124*, 11215. (d) He, J.; Benkö, G.; Korodi, F.; Polívka, T.; Lomoth, R.; Åkermark, B.; Sun, L.; Hagfeldt, A.; Sundström, V. *J. Am. Chem. Soc*. **2002,** *124***,** 4922. (e) Benkö, G.; Myllyperkiö, P.; Pan, J.; Yartsev, A. P.; Sundström, V. *J. Am. Chem. Soc*. **2003,** *125*, 1118. (f) Nishimura, S.; Abrams, N.; Lewis, B. A.; Halaoui, L. I.; Mallouk, T. E.; Benkstein, K. D.; van de Lagemaat, J.; Frank, A. J. *J. Am. Chem. Soc*. **2003**, *125*, 6306. (g) Piotrowiak, P.; Galoppini, E.; Wei, Q.; Meyer, G. J.; Wiewiór, P. *J. Am. Chem. Soc*. **2003**, *125*, 5278. (h) Horiuchi, T.; Miura, H.; Sumioka, K.; Uchida, S. *J. Am. Chem. Soc*. **2004**, *126*, 12218. (i) Tachibana, Y.; Moser, J.-E.; Grätzel, M.; Klug, D. R.; Durrant, J. R. *J. Phys. Chem*. **1996**, *100*, 20056. (j) Huang, S. Y.; Schlichthörl, G.; Nozik, A. J.; Grätzel, M.; Frank, A. J. *J. Phys. Chem. B* **1997**, *101*, 2576. (k) Ellingson, R. J.; Asbury, J. B.; Ferrere, S.; Ghosh, H. N.; Sprague, J. R.; Lian, T.; Nozik, A. J. *J. Phys. Chem. B* **1998**, *102*, 6455. (l) Tachibana, Y.; Haque, S. A.; Mercer, I. P.; Durrant, J. R.; Klug, D. R. *J. Phys. Chem. B* **2000**, *104*, 1198. (m) Pelet, S.; Moser, J.-E.; Grätzel, M. *J. Phys. Chem. B* **2000**, *104*, 1791. (n) Cahen, D.; Hodes, G.; Grätzel, M.; Guillemoles, J. F.; Riess, I. *J. Phys. Chem. B* **2000**, *104*, 2053. (o) Gregg, B. A. *J. Phys. Chem. B* **2003**, *107*, 4688. (p)Yoshihara, T.; Katoh, R.; Furube, A.; Murai, M.; Tamaki, Y.; Hara, K.; Murata, S.; Arakawa, H.; Tachiya, M. *J. Phys. Chem. B* **2004**, *108*, 2643. (q) Lee, J.-J.; Coia, G. M.; Lewis, N. S. *J. Phys. Chem. B* **2004**, *108*, 5269. (r) Coia, G. M.; Lewis, N. S. *J. Phys. Chem. B* **2004**, *108*, 5282.
(4) Nazeeruddin, M. K.; Kay, A.; Rodicio, I.; Humphry-Baker, R.; Müller, E.; Liska, P.; Vlachopoulos, N.; Grätzel, M. *J. Am. Chem. Soc.* **1993**, *115*, 6382.
(5) Grätzel, M. *J. Photochem. Photobiol. A* **2004**, *164*, 3.
(6) Wang, P.; Zakeeruddin, S. M.; Moser, J.-E.; Humphry-Baker, R.; Comte, P.; Aranyos, V.; Hagfeldt, A.; Nazeeruddin, M. K.; Grätzel, M. *Adv. Mater*. **2004**, *16*, 1806.
(7) Wang, P.; Zakeeruddin, S. M.; Comte, P.; Charvet, R.; Humphry-Baker, R.; Grätzel, M. *J. Phys. Chem. B* **2003**, *107*, 14336.
(8) Wang, P.; Zakeeruddin, S. M.; Moser, J.-E.; Nazeeruddin, M. K.; Sekiguchi, T.; Grätzel, M. *Nat. Mater*. **2003**, *2*, 402.
(9) Wang, P.; Zakeeruddin, S. M.; Humphry-Baker, R.; Moser, J.-E.; Grätzel, M. *Adv. Mater*. **2003**, *15*, 2101.

 10.1021/ja042232u CCC: $30.25

ficiency is still desirable.[13] Nevertheless, flexible and lightweight solar cells based on plastic materials are attractive even if their solar conversion yield is moderate, i.e., in the 5 to 10% range. However, for these devices the use of organic solvents is prohibitive, as they would permeate across polymeric cell walls. A very attractive solution to this dilemma consists of employing ionic liquids as nonvolatile and thermally stable electrolytes. Here we report on a new binary ionic liquid electrolyte composed of 1-propyl-3-methylimidazolium iodide and 1-ethyl-3-methylimidazolium tricyanomethanide[14] that reaches an unprecedented 7.4% power conversion efficiency under full air mass (AM) 1.5 sunlight.

Experimental Section

Chemicals. All chemicals and solvents used were of puriss quality. Nitrosyl tetrafluoroborate ($NOBF_4$), [$RuCl_2$(*p*-cymene)$_2$], 4,4′-dicarboxylic acid-2,2′-bipyridine (dcbpy), 4,4′-dinonyl-2,2′-bipyridine (dnbpy), and *N*-methylbenzimidazole (NMBI) were purchased from Aldrich. NMBI was recrystallized from diethyl ether before use. PMII was prepared according to the literature method,[15] and its purity was confirmed by ^{1}H NMR spectrum. Sephadex LH-20 was obtained from Pharmacia (Sweden). TiO_2 particles of 400 nm were received as a gift from CCIC (Japan).

ATR-FTIR Measurements. The spectra for all the samples were measured using a Digilab FTS 7000 FTIR spectrometer fitted with a DTGS detector. All the data reported here were taken with the "Golden Gate" 45 diamond anvil ATR accessory. Spectra were derived from 64 scans at a resolution of 2 cm^{-1}. Some of the spectra show artifacts due to attenuation of light by the diamond window in the 2000 to 2350 cm^{-1} region. TiO_2 particles of 20 nm were deposited by doctor blading directly onto the diamond window and further annealed at 250 °C to remove volatile dispersants. A higher temperature is not recommended so as to avoid destroying the glue holding the diamond support on the ATR top plate. This gives a mesoporous film that is about 3 μm thick, which is more than adequate for the optical sampling depth of the ATR technique that is at most about 1.5 μm.[16] This sampling depth depends on the sample refractive index, porosity, etc. The TiO_2 film was first cleaned in situ with a basic aqueous solution (pH = 11) to remove surface carbonate and then rinsed with water. The mixed solvent of acetonitrile and *tert*-butyl alcohol (volume ratio 1:1) was introduced and allowed to equilibrate for about 30 min or until repetitive scans remained unchanged. The schematic ATR-FTIR setup to monitor the dynamics of dye uptake onto nanocrystalline TiO_2 film is shown in Figure 1.

A reference FTIR spectrum of the corresponding TiO_2/solvent was recorded prior to the introduction of the adsorbate solution. Spectra were recorded, with reference to this baseline spectrum, over a series of time intervals while the dye solution circulated above the film. At the dye concentrations used, interference due to the bulk dye solution was less than 1%.

Preparation and Stability of the Oxidized Form of the Sensitizer. A 10 μL aliquot of a freshly prepared solution of $NOBF_4$ (4 mM) was added to 2 mL of the Z-907Na dye solution (27 μM) installed in a

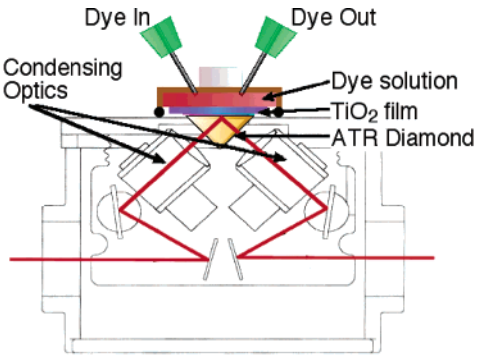

Figure 1. Schematic ATR-FTIR setup to monitor the dynamics of dye uptake onto nanocrystalline TiO_2 film.

UV−vis spectrophotometer. The kinetics was monitored continuously at 770 nm while stirring at 25 °C. The mixture of acetonitrile and *tert*-butyl alcohol (volume ratio 9:1) was used as solvent for this experiment.

Conductivity Measurements. A CDM210 conductivity meter (Radiometer Analytical, SAS, France) was used to measure conductivities. The CDC749 conductivity cell (Radiometer Analytical, SAS, France) with a nominal cell constant of 1.70 cm^{-1} was calibrated with 0.1 M KCl aqueous solution prior to the experiments. A DT Hetotherm cycle heat pump (Heto, Denmark) was used to control the temperature.

Voltammetric and Photoelectrochemical Measurements. Voltammetric data were recorded at room temperature on an Autolab P20 electrochemical workstation (Eco Chimie, Netherlands). A three-electrode electrochemical cell was used for the measurements of the formal redox potentials of sensitizers in DMF. A Pt ultramicroelectrode, a Pt foil, and an Ag/AgCl/KCl_{sat} were employed as working, counter, and reference electrodes, respectively. Supporting electrolyte: 0.1 M tetrabutylammonium hexafluorophosphate. Due to the possible liquid junction potential, the used reference electrode was calibrated by measuring the redox potential of ferrocene dissolved in DMF. The redox potentials measured against the calibrated Ag/AgCl/KCl_{sat} electrode were converted to the NHE reference scale. A two-electrode electrochemical cell, consisting of a 5.0 μm radius Pt ultramicroelectrode as working electrode and a Pt foil as counter electrode, was used for measurements of the iodide diffusion coefficient and iodide flux. Photoelectrochemical data were collected as reported previously.[10b]

Nanosecond Laser Transient Absorbance Measurements. Dye-coated, 8 μm thick transparent nanocrystalline TiO_2 films were excited by nanosecond laser pulses produced by a Continuum Powerlite 7030 frequency-doubled Q-switched Nd:YAG laser (λ = 532 nm, 30 Hz repetition rate, pulse width at half-height of 7 ns, pulse fluence of 200 μJ cm^{-2}). The probe light from a Xe arc lamp was passed through a monochromator, various optical elements, the sample, and a second monochromator before being detected by a fast photomultiplier tube. Typically, averaging over 1000 laser shots was necessary to get satisfactory signal/noise levels.

Synthesis of NaRu(4-carboxylic acid-4′-carboxylate)(4,4′-dinonyl-2,2′-bipyridine)(NCS)$_2$ (Z-907Na). $RuCl_2$(*p*-cymene)$_2$ (1 g, 1.6 mmol) and dnbpy (1.33 g, 3.2 mmol) were dissolved in DMF (500 mL). The reaction mixture was heated to 60 °C under nitrogen for 4 h with constant stirring. Subsequently, dcbpy (0.8 g, 3.2 mmol) was added to this reaction flask and the reaction mixture was refluxed at 140 °C for 4 h. Finally, an excess of NH_4NCS (130 mmol) was added to the reaction mixture and the reflux continued for another 4 h. The reaction mixture was cooled to room temperature, and the solvent was removed by using a rotary evaporator under vacuum. Water was added to the flask, and the insoluble solid was collected on a sintered glass crucible by suction filtration. The solid was washed with distilled water and diethyl ether and then dried under vacuum. The crude complex was dissolved in basic methanol (NaOH) and purified on a Sephadex LH-20 column with methanol as eluent. The collected main band was

(10) (a) Wang, P.; Zakeeruddin, S. M.; Comte, P.; Exnar, I.; Grätzel, M. *J. Am. Chem. Soc*. **2003**, *125*, 1166. (b) Wang, P.; Zakeeruddin, S. M.; Moser, J.-E.; Grätzel, M. *J. Phys. Chem. B* **2003**, *107*, 13280. (c) Wang, P.; Zakeeruddin, S. M.; Humphry-Baker, R.; Grätzel, M. *Chem. Mater*. **2004**, *16*, 2694.
(11) Nusbaumer, H.; Zakeeruddin, S. M.; Moser, J.-E.; Grätzel, M. *Chem. Eur. J*. **2003**, *9*, 3756.
(12) Schmidt-Mende, L.; Zakeeruddin, S. M.; Grätzel, M. *Appl. Phys. Lett.* **2005**, *86*, 013504.
(13) Service, R. F. *Science* **2003**, *300*, 1219.
(14) Yoshida, Y.; Muroi, K.; Otsuka, A.; Saito, G.; Takahashi, M.; Yoko, T. *Inorg. Chem*. **2004**, *43*, 1458.
(15) Bonhôte, P.; Dias, A. P.; Armand, M.; Papageorgiou, N.; Kalyanasundaram, K.; Grätzel, M. *Inorg. Chem*. **1996**, *35*, 1168.
(16) McQuillan A. J. *Adv. Mater*. **2001**, *13*, 1034.

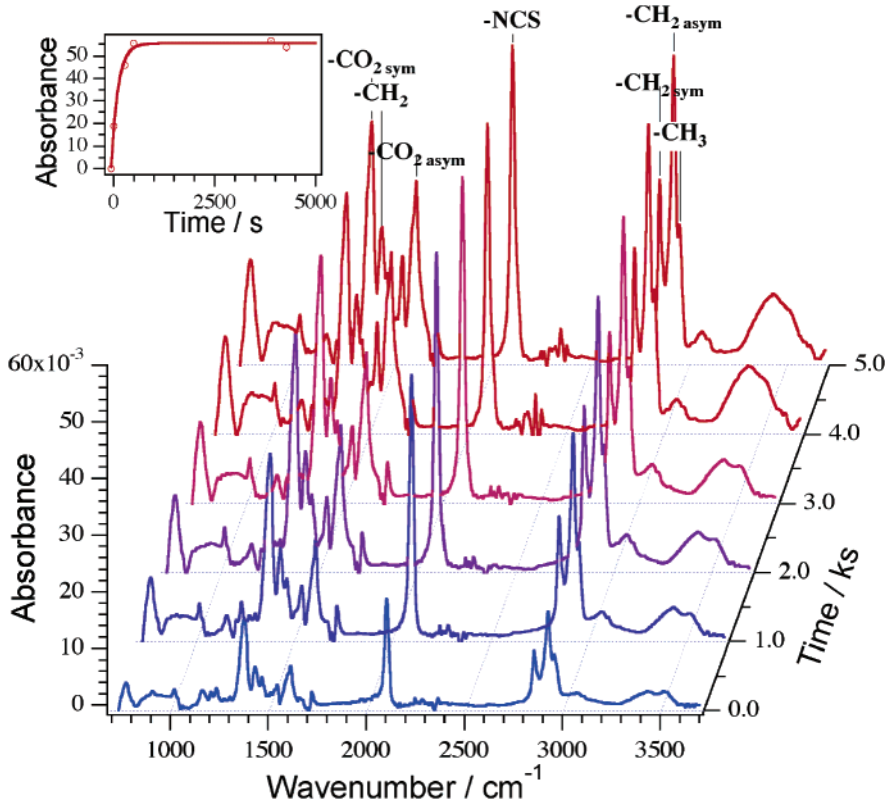

Figure 2. Dynamic ATR-FTIR spectra of staining of the TiO_2 nanocrystalline film with the Z-907Na sensitizer. Dye solution: 300 μM Z-907Na in acetonitrile and *tert*-butyl alcohol (volume ratio 1:1). The temporal evolution of the thiocyanate absorbance (mOD) is shown in the upper left corner.

concentrated and then slowly titrated with an acidic methanol solution (HNO_3) to pH 4.8. The precipitate was collected on a sintered glass crucible by suction filtration and dried. ^{1}H NMR (δ_H/ppm in CD_3OD/NaOH): 9.55 (d, 1H), 9.35 (d, 1H), 9.05 (s, 1H), 8.85 (s, 1H), 8.5 (s, 1H), 8.35 (s, 1H), 8.20 (d, 1H), 7.70 (dd, 2H), 7.60 (d, 1H), 7.40 (d, 1H), 7.05 (d, 1H), 3.00 (t, 2H), 2.75 (t,2H) 1.9−1.3 (m, 28H), 0.8 (t, 6H). Anal. Calcd for $NaRuC_{42}H_{51}N_6O_6S_2 \cdot 3H_2O$: C, 53.33; H, 6.03; N, 8.90. Found; C, 53.75; H, 6.00; N, 9.02. The formal redox potential of Z-907Na in DMF measured by square-wave voltammetry is 0.87 V vs NHE, while those of the completely protonated and deprotonated types are at 0.96 and 0.78 V, respectively.

Synthesis of EMITCM. Solutions of potassium tricyanomethanide (5.56 g, 43 mmol) in 50 mL of acetonitrile and EMIBr[15] (5.48 g, 29 mmol) in 10 mL of acetonitrile were mixed and stirred at room temperature for 18 h. The precipitated potassium bromide was filtered off, and the solvent was removed under reduced pressure. Dichloromethane (50 mL) was added to the residue and kept at 2 °C for 16 h. The separated solid was filtered off, and the filtrate was washed with 5 mL of water and evaporated on a rotary evaporator. The traces of water were removed by an azeotropic distillation with toluene. EMITCM was dried under reduced pressure (0.01 Torr). Yield: 4.49 g (77%). Anal. Calcd for $C_{10}H_{11}N_5$: C, 59.69; H, 5.51; N, 34.80; Br, 0.00. Found: C, 60.05; H, 5.45; N, 34.44; Br, 0.00.

Fabrication of Photovoltaic Devices. The mesoporous TiO_2 film used for the photoanodes consisted of two layers. A transparent, high surface area layer (10 μm) of 20 nm sized TiO_2 particles was first printed on the fluorine-doped SnO_2 conducting glass electrode and further coated by a 4 μm thick second layer of 400 nm light scattering anatase particles. The detailed fabrication procedures for the nanocrystalline TiO_2 film and the assembly of complete, hot-melt sealed cells have been described elsewhere.[7] The TiO_2 electrode was stained by immersing it into a solution of 300 μM Z-907Na sensitizer and 300 μM 3-phenylpropionic acid coadsorbent in acetonitrile and *tert*-butyl alcohol (volume ratio 1:1) at room temperature for 12 h.

Stability Tests. Solar cells covered with a 50 μm thick polyester film (Preservation Equipment Ltd, UK) as a 400 nm UV cutoff filter were irradiated at open circuit under a Suntest CPS plus lamp (ATLAS GmbH, 100 mW cm^{-2}) in ambient air at 60 °C. Photoelectrochemical measurements were carried out room temperature after allowing the cells to cool and equilibrate for a few hours.

Results and Discussion

Dynamic ATR-FTIR Studies to Monitor Dye Uptake. The rate of dye uptake by the mesoporous TiO_2 film is a very important diagnostic for device fabrication. In Figure 2, the adsorption rate is monitored by ATR-FTIR spectroscopy. The IR absorption bands augment with time to achieve a constant value after about 15 min for a 3 μm film using the strong thiocyanate peak as marker.

The other advantage of monitoring this process is that the IR spectrum provides information on a molecular scale as to the state of the dye when attached to the surface. The ATR-FTIR spectrum of the dyed mesoporous oxide electrode can yield structural information of the adsorbed species at the interface. The presence of Z907Na is identified by the single peak at 2103 cm^{-1} due to the presence of the −NCS group. Other characteristic peaks are at 1612 and 1387 cm^{-1} due to the asymmetric and symmetric carboxylate group and the sharp pyridine ring modes at 1543, 1437, 1236, and 1019 cm^{-1}. The saturated hydrocarbon chains are easily identified from their C−H stretch modes in the 2800−3000 cm^{-1} region. Peaks at 2855 and 2920 cm^{-1} are due to the symmetric and asymmetric $-CH_2-$ stretch vibrations. The corresponding CH_3- peaks are observed at 2955 and ∼2870 cm^{-1}. The relative intensities of the CH_3- peak to the $-CH_2-$ peaks agree well with the expected pattern for a C_9 chain length.

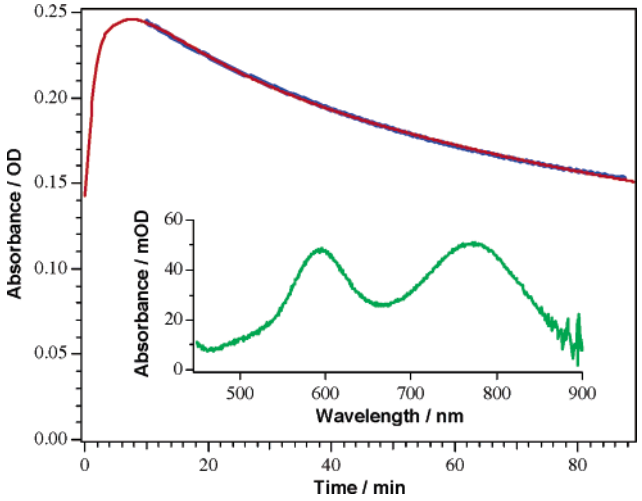

Figure 3. Time dependence for the evolution and decay of the oxidized form of Z-907Na in solution. The inset shows the oxidized form derived from the subtraction of the starting material at $t \approx 0$.

Despite the observation of trace amounts of the carbonyl peak at 1720 cm^{-1}, most of the carboxlates are involved in attachment to the TiO_2 surface via a bidentate surface attachment, since the adsorbate solution spectrum showed the presence of both the acid $-COOH$ and a carboxylate anion from the $-CO_2Na$. Dye adsorption on TiO_2 must occur promptly followed by rapid exchange of the proton on the surface to show only the carboxylate functionalities.

The peak at ~774 cm^{-1} is also a strong diagnostic for surface adsorption. It is always present upon dye uptake and is probably due to changes in the surface TiO_2 bonds of the anatase crystallites.[17] The amount of surface-associated water is seen to increase due to the observed broad peak at 3430 cm^{-1}.[9] Dye uptake appears to aid the amount of water associated with this interface. This is partly due to the release of protons from the dye to the surface upon adsorption but also partly due to the water that is present in the solvent system used.

Lifetime of the Oxidized State of Sensitizer. Upon addition of the oxidant, the Z-907Na peaks immediately shift to the red with the lowest MLCT being at 550 nm. This peak position is analogous to the Z-907 with two protons, which may be caused by a strong affinity of the nitrosyl cation to the carboxylate functionality.

By monitoring the absorption change at 770 nm, the formation of the oxidized form of Z-907Na is seen to occur over the first 8−10 min after the addition of the oxidant. This point corresponds to about a 20% decrease in the 550 nm peak of the sensitizer in the initial presence of $NOBF_4$. The insert in Figure 3 shows the spectrum of the oxidized sensitizer. This shows two broad peaks with maxima at 594 and 768 nm. After the zenith, the oxidized form starts to decay with a half-life of 53 min. The slow decay was not investigated in the context of the present article. Compared with the standard N3 dye the lifetime for the oxidized state of the Z-907Na is remarkably prolonged, and this is likely to arise from the lower oxidation potential of the Z-907 compared to the N3 dye.

Correlation between Photocurrent and Iodide Concentration in Binary Ionic Liquid Electrolytes. Ionic liquid electrolytes[18−22] are normally more viscous in contrast to conventional organic solvent based electrolytes. In exploring their applicability for nanocrystalline dye-sensitized solar cells with a considerable high current density of over 15 mA cm^{-2}, the mass transport of triiodide[23−25] has been previously considered as a limiting factor because of its lower diffusion coefficient and lower concentration in electrolytes compared with those for iodide. Initial results obtained by simply replacing the organic solvent with some ionic liquids were disappointing.[23] An impressive 6% efficiency[10a] under AM 1.5 full sunlight was achieved by employing the amphiphilic Z-907 sensitizer in conjunction with an ionic liquid containing very high iodine concentration, i.e., by doping pure 1-propyl-3-methylimidazolium iodide (PMII) having a viscosity of about 880 cP with 0.5 M I_2. At an iodine concentration below 0.2 M, mass transport of triiodide does become the main limitation in this type of thin-layer electrochemical cell. For comparison a device employing the same Z-907Na sensitizer and an acetonitrile-based electrolyte gave a conversion efficiency of 9.5% in full AM 1.5 sunlight, the short-circuit photocurrent density (J_{sc}), open-circuit photovoltage (V_{oc}), and fill factor (*ff*) of this being 16.7 mA cm^{-2}, 753 mV, and 0.75, respectively.

Replacing part of the iodide in the PMII by some weakly coordinating anions can lower the viscosity of the ionic liquid.[26] Thus, mixtures of PMII with 1-ethyl-3-methylimidazolium dicyanoamide and 1-ethyl-3-methylimidazolium thiocyanate achieve conversion efficiencies above 6.0% in full sunlight.[10b,c] However a high mole fraction of PMII is required in these binary systems to maintain photovoltaic performance even if the triodide concentration is sufficient to avoid diffusion limitation of the photocurrent. This unexpected behavior is now analyzed

(17) (a) Shao, L.; Zhang, L.; Chen, M.; Lu, H.; Zhou M. *Chem. Phys. Lett.* **2001**, *343*, 178. (b) Dobson, K. D.; McQuillan, A. J. *Langmuir* **1997**, *13*, 3392.

(18) (a) Xu, W.; Angell, C. A. *Science* **2003**, *302*, 422. (b) Yoshizawa, M.; Xu, W.; Angell, C. A. *J. Am. Chem. Soc.* **2003**, *125*, 15411. (c) Xu, W.; Cooper, E. I.; Angell, C. A. *J. Phys. Chem. B* **2003**, *107*, 6170. (d) Hayashi A.; Yoshizawa, M.; Angell, C. A.; Mizuno, F.; Minami, T.; Tatsumisago, M. *Electrochem. Solid State Lett.* **2003**, *6*, E19.

(19) (a) Ito K.; Nishina, N.; Ohno, H. *Electrochim. Acta* **2000**, *45*, 1295. (b) Ohno, H.; Yoshizawa, M. *Solid State Ionics* **2002**, *154−155*, 303. (c) Ogihara, W.; Yoshizawa, M.; Ohno, H. *Chem. Lett.* **2002**, 880. (d) Yoshizawa, M.; Ohno, H. *Chem. Commun.* **2004**, 1828. (e) Ogihara, W.; Yoshizawa, M.; Ohno, H. *Chem. Lett.* **2004**, *33*, 1022.

(20) (a) Fuller, J.; Breda, A. C.; Carlin, R. T. *J. Electrochem. Soc.* **1997**, *144*, L67. (b) Fuller, J.; Carlin, R. T.; Osteryoung, R. A. *J. Electrochem. Soc.* **1997**, *144*, 3881. (c) Kosmulski, M.; Osteryoung, R. A.; Ciszkowska, M. *J. Electrochem. Soc.* **2000**, *147*, 1454. (d) Sutto, T. E.; De Long, H. C.; Trulove, P. C. *Z. Naturforsch. A* **2002**, 57, 839.

(21) (a) Lu, W.; Fadeev, A. G.; Qi, B.; Smela, E.; Mattes, B. R.; Ding, J.; Spinks, G. M.; Mazurkiewicz, J.; Zhou, D.; Wallace, G. G.; MacFarlane, D. R.; Forsyth, S. A.; Forsyth, M. *Science* **2002**, *297*, 983. (b) Ue, M.; Takeda, M.; Toriumi, A.; Kominato, A.; Hagiwara, R.; Ito, Y. *J. Electrochem. Soc.* **2003**, *150*, A499. (c) Fukushima, T.; Kosaka, A.; Ishimura, Y.; Yamamoto, T.; Takigawa, T.; Ishii, N.; Aida, T. *Science* **2003**, *300*, 2072. (d) Noda, A.; Susan, M. A. B. H.; Kudo, K.; Mitsushima, S.; Hayamizu, K.; Watanabe, M. *J. Phys. Chem. B* **2003**, *107*, 4024. (e) Sakaebe, H.; Matsumoto, H. *Electrochem. Commun.* **2003**, *5*, 594. (f) de Souza, R. F.; Padilha, J. C.; Gonçalves, R. S.; Dupont, J. *Electrochem. Commun.* **2003**, *5*, 728. (g) Shin, J.-H.; Hendenson, W. A.; Passerini, S. *Electrochem. Commun.* **2003**, *5*, 1016. (h) Sato, T.; Masuda, G.; Takagi, K. *Electrochim. Acta* **2004**, *49*, 3603. (i) Holzapfel, M.; Jost, C.; Novák, P. *Chem. Commun.* **2004**, 2098. (j) Balducci, A.; Bardi, U.; Caporali, S.; Mastragostino, M.; Soavi, F. *Electrochem. Commun.* **2004**, *6*, 566.

(22) (a) Matsumoto, H.; Matsuda, T.; Tsuda, T.; Hagiwara, R.; Ito, Y.; Miyazaki, Y. *Chem. Lett.* **2001**, 26. (b) Murai, S.; Mikoshiba, S.; Sumino, H.; Kato, T.; Hayase, S. *Chem. Commun.* **2003**, 1534. (c) Paulsson, H.; Hagfeldt, A.; Kloo, L. *J. Phys. Chem. B* **2003**, *107*, 13665.

(23) Papageorgiou, N.; Athanassov, Y.; Armand, M.; Bonhôte, P.; Pettersson, H.; Azam, A.; Grätzel, M. *J. Electrochem. Soc.* **1996**, *143*, 3099.

(24) (a) Kubo, W.; Kambe, S.; Nakade, S.; Kitamura, T.; Hanabusa, K.; Wada, Y.; Yanagida, S. *J. Phys. Chem. B* **2003**, *107*, 4374. (b) Kubo, W.; Kitamura, T.; Hanabusa, K.; Wada, Y.; Yanagida, S. *Chem. Commun.* **2002**, 374.

(25) Wang, P.; Zakeeruddin, S. M.; Grätzel, M.; Kantlehner, W.; Mezger, J.; Stoyanov, E. V.; Scherr, O. *Appl. Phys. A* **2004**, *79*, 73.

(26) Wasserscheid, P.; Welton, T. *Ionic Liquids in Synthesis*; Wiley: Weinheim, 2002.

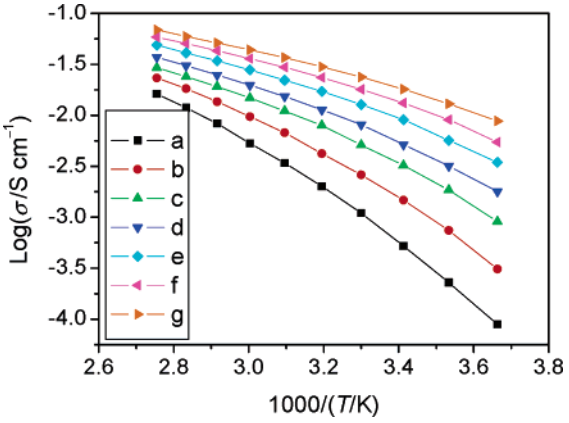

Figure 4. Conductivity−temperature plots in the Arrhenius coordinate for (a) PMII, (g) EMITCM, and binary mixtures (b−f) of PMII and EMITCM at different ratios. PMII volume percentage: (b) 80%; (c) 65%; (d) 50%; (e) 35%; (f) 20%.

in more detail using mixtures of PMII with the ionic liquid EMITCM, whose viscosity is 18 cP at 22 °C.[14]

As stated in the empirical Walden's rule ($\Lambda\eta$ = constant), the product of the equivalent conductivity (Λ) and the viscosity (η) of the solvent for a particular electrolyte at a given temperature should be constant, where Λ can be represented by $\sigma M/d$ (σ, conductivity; M, formula weight; d, density) for ionic liquids.[27] Recent work by Angell et al.[18c] has shown that the Walden rule applies rather well to a pure ionic liquid. As shown in Figure 4, reducing the volume ratio of PMII by mixing with EMITCM increases the conductivity, its value at 20 °C augmenting ~9 times from 1.47 to 13.17 mS s^{-1} when the percentage of PMII was reduced from 80 to 20%. Since there is not much difference in the M/d ratio for PMII and EMITCM, this remarkable increase in conductivity is due to enhanced ionic mobility that stems from the decreased viscosity. As shown in Figure S1, the conductivity−temperature data for all these mixtures of ionic liquids fit well with the Vogel−Fulcher−Tammann (VFT) equation.[28]

The recombination of the injected electron with oxidized sensitizer is a loss channel reducing the photocurrent of the DSC. To avoid this current loss, regeneration of the dye by electron donation from the iodide has to be sufficiently fast to intercept the back reaction. The limiting anodic current was measured by ultramicroelectrode technique. Steady-state voltammograms for the iodide oxidization processes are presented in Figure 5A. The apparent iodide diffusion coefficient D_{app} of iodide can be calculated from the anodic steady-state currents (I_{ss}) according to the equation $I_{ss} = 4ncaFD_{app}$, where n is the electron transferred in the oxidation event, F is the Faraday constant, a is the radius of ultramicroelectrode, and c is the bulk concentration of electroactive species.[29] Figure 5B shows that D_{app} increases from 5.24×10^{-7} to 7.37×10^{-7} cm^2 s^{-1} by lowering the volume percentage of PMII from 80 to 20%. The apparent discrepancy in the variation of conductivity (or viscosity) and diffusion coefficient of iodide can be rationalized by the

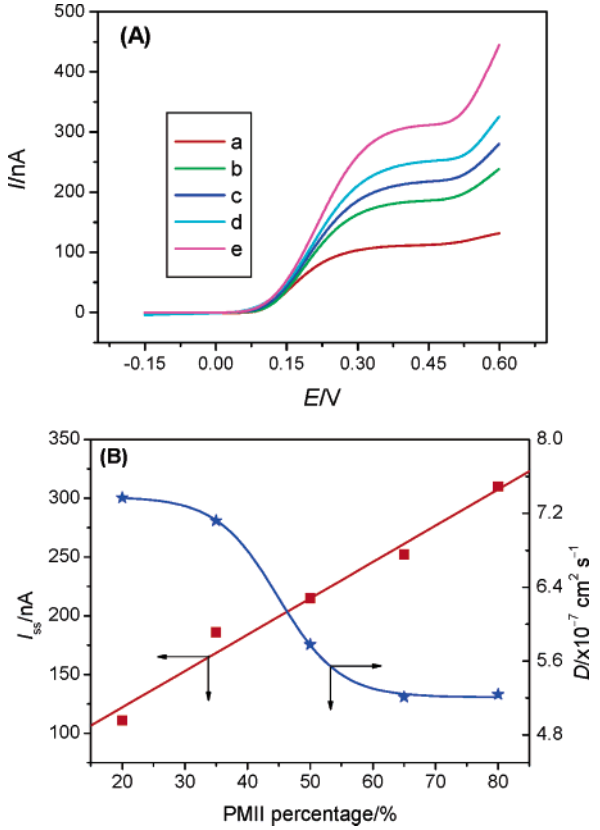

Figure 5. (A) Steady-state voltammograms of a Pt ultramicroelectrode in the binary mixtures of PMII and EMITCM. PMII volume percentage: (a) 20%; (b) 35%; (c) 50%; (d) 65%; (e) 80%. (B) Dependence of steady-state current and iodide diffusion coefficient on the volume percentage of PMII in the binary mixtures.

Dahms−Ruff equation[30] ($D_{APP} = D_{PHYS} + D_E = D_{PHYS} + k_{EX}\delta^2 c/6$, where D_{PHYS} and D_E are the physical and electron exchange diffusion coefficients, respectively, k_{EX} is the rate constant of electron exchange, and c and δ are the concentration and average center-to-center distances between redox species, respectively). The D_E term behaves in a different manner from the viscosity-dependent D_{PHYS} term. The high packing density of iodide favors a Grotthus-like exchange mechanism, leading to a higher D_E.

For photovoltaic studies the concentration of iodine was kept constant (0.2 M) in the above binary ionic liquid electrolytes. As the concentration of PMII increases from 20 to 50%, the trend of photocurrent density and efficiency for devices measured at AM 1.5 full sunlight (100 mW cm^{-2}) is consistent with the change of the iodide diffusion flux rather than the diffusion coefficient (Figures 5B and 6). Thus the iodide diffusional flux rather than its diffusion coefficient determines the performance of nanocrystalline dye-sensitized solar cells. Even at 50% of PMII, the diffusion flux of iodide is still much smaller than that in a MPN-based electrolyte, yielding a J_{sc} of 14.2−15.2 mA cm^{-2}.[7]

However, a further increase in the PMII concentration from 50 to 80% resulted in a decrease in photocurrent density and device efficiency. This cannot be ascribed to triiodide mass transfer problems, as this trend was also observed at a lower light intensity, i.e., 9.5 mW cm^{-2}.

(27) Bockris, J. O'M.; Reddy, A. K. N. *Modern Electrochemistry*, Vol. 1, 2nd ed.; Plenum: New York, 1998.
(28) (a) Vogel, H. *Physik. Z.* **1921**, *22*, 645. (b) Fulcher, G. S. *J. Am. Ceram. Soc.* **1925**, *8*, 339. (c) Tammann, V. G.; Hesse, W. *Z. Anorg. Allg. Chem.* **1926**, *156*, 245. (d) Angell, C. A.; Bressel, R. D. *J. Phys. Chem.* **1972**, *76*, 3244.
(29) Bard, A. J.; Faulkner, L. R. *Electrochemical Methods: Fundamentals and Applications*, 2nd ed.; Wiley: Weinheim, 2001.
(30) (a) Dahms, H. *J. Phys. Chem.* **1968**, *72*, 362. (b) I. Ruff, I.; Friedrich, V. J. *J. Phys. Chem.* **1971**, *75*, 3297. (c) Ruff, I.; Friedrich, V. J.; Csillag, K. *J. Phys. Chem.* **1972**, *76*, 162.

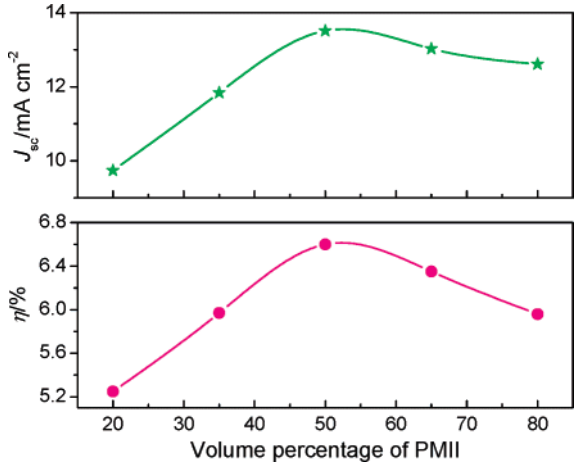

Figure 6. Dependence of photocurrent density and power conversion efficiency of devices under the AM 1.5 full sunlight (100 mW cm^{-2}) on the volume percentage of PMII. The iodine concentration is kept at 0.2 M.

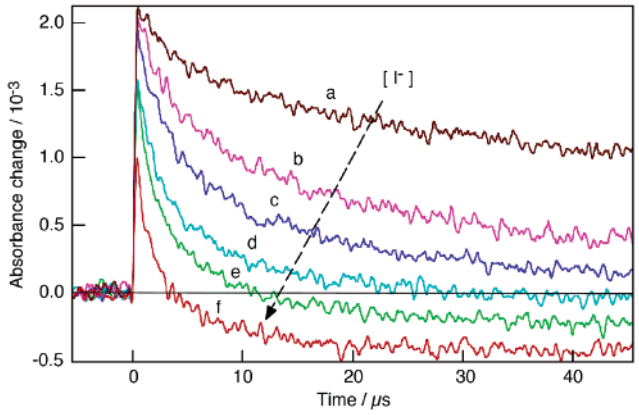

Figure 7. Transient absorbance at 630 nm of dye-sensitized transparent TiO_2 films in binary mixtures of PMII and EMITCM. The iodide concentration was increased from 0 to 5.8 M by raising the PMII volume percentage: (a) 0%; (b) 5%; (c) 11%; (d) 23%; (e) 45%; (f) 100%.

Laser transient absorbance measurements were performed to scrutinize the adverse effect of very high iodide concentration. Since iodide is also capable of interacting with the excited sensitizer, it can create a competing deactivation pathway for the excited sensitizer.[31] Earlier studies have shown that excited $[Ru(bpy)_3]^{2+}$ with its redox potential at +0.83 V (vs NHE) readily undergoes one-electron reduction in the presence of a donor such as some metal ions and amines.[32] Figure 7 displays the temporal evolution of the absorbance measured at 630 nm of a transparent dye-sensitized TiO_2 film upon pulsed laser excitation (wavelength, 532 nm; pulse duration, 7 ns; pulse fluence, 200 μJ cm^{-2}). At the probe wavelength of 630 nm, both the ground (S) and the oxidized sensitizer (S^+) absorb light with extinction coefficients of 2.4×10^3 and 4.8×10^3 M^{-1} cm^{-1}, respectively. The ultrafast charge injection (eq 1) thus involves the appearance of a positive transient signal. In the absence of iodide donor, this signal decays (trace a) due to back

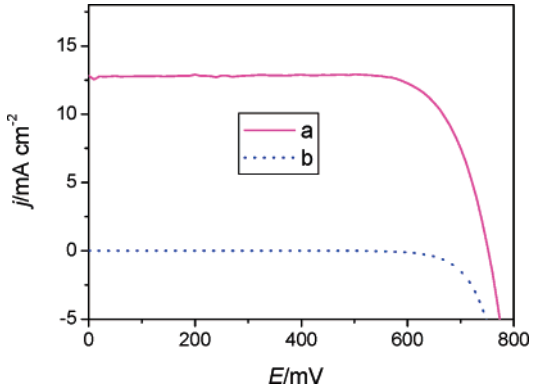

Figure 8. Current density−potential curves of devices with optimized binary ionic liquid electrolyte (a) under the AM 1.5 full sunlight and (b) in the dark. Cell area tested with mask: 0.158 cm^2.

electron transfer from the conduction band to the oxidized dye (eq 2).

$$S^*|TiO_2 \rightarrow S^+|TiO_2 + e^-_{cb}(TiO_2) \quad (1)$$

$$S^+|TiO_2 + e^-_{cb}(TiO_2) \rightarrow S|TiO_2 \quad (2)$$

$$S^+|TiO_2 + 2I^- \rightarrow S|TiO_2 + I_2^{-\bullet} \quad (3)$$

$$S^*|TiO_2 + 2I^- \rightarrow S^-|TiO_2 + I_2^{-\bullet} \quad (4)$$

Increasing the iodide concentration is expected to cause an acceleration of dye regeneration (eq 3). Indeed the decay of S^+ transient absorbance was observed to be faster in binary mixtures of ionic liquids when the PMII volume fraction was augmented (traces b−f). In the case of high PMII percentages, a clear bleaching of the sensitizer's ground state was observed at the end of the regeneration process (eq 3). This feature, combined with the observation of changes in the blue-green part (450 nm $< \lambda <$ 550 nm) of the transient spectra recorded at high PMII contents (not shown), provided evidence for the formation of a new species that was identified as being the reduced dye (S^-) formed by reaction 4.[33] Further transient laser experiments have shown that S^- does not actually inject an electron into TiO_2, but decays only through a slow reaction with I_3^- with $t_{1/2} =$ ~1 ms. Detailed nanosecond and femtosecond laser studies of the kinetic competition between electron injection from dye excited states and their reductive quenching in iodide melts, as well as of the implications of dye aggregates on the surface, will be reported in a forthcoming publication.[33] Calculations based on the extent of the bleaching measured at 630 nm and extinction coefficients show that approximately 25% of the sensitizer's excited states do experience reductive quenching in the presence of pure PMII. This means that a non-negligible fraction of the potential photocurrent could be lost through the reductive quenching route in the presence of high PMII contents.

On the basis of the above results, 0.5 M NMBI was added as a Lewis base to the mixture of PMII and EMITCM at 1:1 volume ratio to enhance the device photovoltage. Figure 8 presents the current density−voltage characteristics of a device with the optimized binary ionic liquid electrolyte under the illumination of AM 1.5 sunlight at 100 mW cm^{-2}. The

(31) (a) Nasr, C.; Hotchandani, S.; Kamat, P. V. *J. Phys. Chem. B* **1998**, *102*, 4944. (b) Thompson, D. W.; Kelly, C. A.; Farzad, F.; Meyer, G. J. *Langmuir* **1999**, *15*, 650. (c) Bergeron, B. V.; Meyer, G. J. *J. Phys. Chem. B* **2003**, *107*, 245.

(32) (a) Baxendale, J. H.; Fiti, M. *J. Chem. Soc., Dalton Trans*. **1972**, 1995. (b) Creutz, C.; Sutin, N. *J. Am. Chem. Soc*. **1976**, *98*, 6384. (c) Meisel, D.; Matheson, M. S.; Mulac, W. A.; Rabani, J. *J. Phys. Chem*. **1977**, *81*, 1449. (d) Baggott, J. E. *J. Phys. Chem*. **1983**, *87*, 5223. (e) Kitamura, N.; Kim, H.-B.; Okano, S.; Tazuke, S. *J. Phys. Chem.* **1989**, *93*, 5750.

(33) Wenger, B.; Teuscher, J.; Zakeeruddin, S. M.; Grätzel, M.; Moser, J. E, manuscript in preparation.

Table 1. Device Parameters Based on the Optimized Ionic Liquid Electrolyte under Different Incident Light Intensities[a]

P_{in}/mW cm^{-2}	J_{sc}/mA cm^{-2}	V_{oc}/mV	P_{max}/mW cm^{-2}	*ff*	η/%
30	4.11	722	2.3	0.784	7.8
52	7.08	734	4.0	0.775	7.7
100	12.81	752	7.4	0.764	7.4

[a] The spectral distribution of the lamp simulates air mass 1.5 solar light. Incident power intensity: P_{in}; short-circuit photocurrent density: J_{sc}; open-circuit photovoltage: V_{oc}; maximum electrical output power density: P_{max}; fill factor: $ff = P_{max}/P_{in}$; total power conversion efficiency: η. Cell active area: 0.158 cm^2.

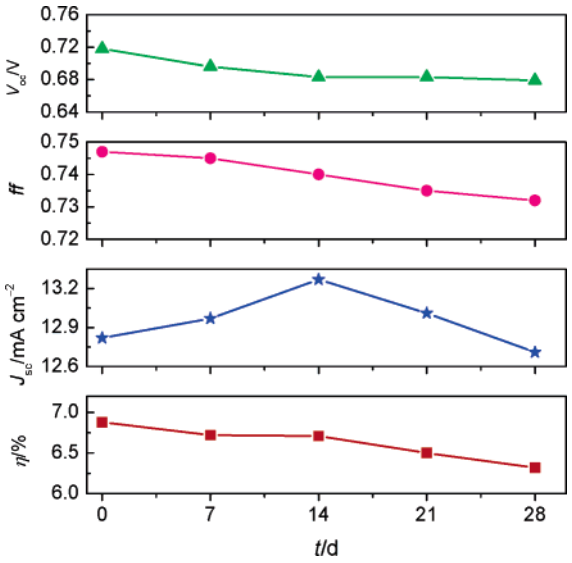

Figure 9. Evolution of photovoltaic parameters during the one sun visible light soaking at 60 °C.

photovoltaic parameters (J_{sc}, V_{oc}, *ff*, and η) were measured to be 12.81 mA cm^{-2}, 752 mV, 0.764, and 7.4%, respectively. This is the highest efficiency that has been achieved so far under the AM 1.5 full sunlight by solvent-free ionic liquid electrolytes with the iodide/triiodide redox couple. As listed in Table 1, at low light intensities overall power conversion efficiency is over 7.5%. However, due to the constraints of rapid dye regeneration and no reductive quenching, a difference in photocurrent density of 3.9 mA cm^{-2} was observed between the present device and that with an acetonitrile solvent based electrolyte as aforementioned.

Cell Stability. The present study permits for the first time the comparison of the lifetime of the oxidized sensitizer in the absence and presence of iodide as the regenerating electron donor. Figure 3 shows that without regenerating agent the oxidized sensitizer survives for 53 min, while in the presence of 23% PMII its lifetime is reduced to 3 μS, as shown by curve d in Figure 7. Thus the kinetic branching ratio of the degradation and regeneration reaction is 10^9. This is about 10 times higher than the value required to ascertain 20 years' operation under natural conditions.

As an example, the evolution of photovoltaic parameters of a DSC with the binary ionic liquid electrolyte is presented in Figure 9. In the first two weeks, a small drop in photovoltage and fill factor was partially compensated by an increase in photocurrent. During the second phase of the light soaking process a ~10% decrease of the short-circuit photocurrent was witnessed, while the open-circuit photovoltage remained stable.

Conclusions

In summary, ATR-FTIR was employed as a powerful technique to monitor the dynamics of the dye uptake process. Additionally, this heteroleptic Z-907Na sensitizer showed a relatively long lifetime of its oxidized state, which is highly desirable for practical application. For the first time 7.4% power conversion efficiency at full sunlight has been achieved for photovoltaic devices with solvent-free ionic liquid electrolytes based on the iodide/triiodide redox couple. In ionic liquid electrolytes a high concentration of iodide is essential for fast dye regeneration; however it will cause enhancement in rate of reductive quenching of excited sensitizer, creating another channel of deactivation.

Acknowledgment. The authors would like to thank P. Comte and R. Charvet for the film fabrication and T. Koyanagi (CCIC, Japan) for a free sample of the 400 nm sized light scattering anatase particles. Financial support by the Swiss Science Foundation under National Program No. 47 and the European Office of the U.S. Air Force under Contract No. F61775-00-C0003 is gratefully acknowledged.

Supporting Information Available: Conductivity−temperature data in the VFT coordinate. This material is available free of charge via the Internet at http://pubs.acs.org.

JA042232U